Spectrochimica Acta Part A 78 (2011) 360–370

Contents lists available at ScienceDirect

Spectrochimica Acta Part A: Molecular and Biomolecular Spectroscopy

journal homepage: www.elsevier.com/locate/saa

Structural studies and anticancer activity of a novel (N_6O_4) macrocyclic ligand and its Cu(II) complexes

Hanaa A. El-Boraey, Sanaa M. Emam, Dina A. Tolan, Ahmed M. El-Nahas*

Department of Chemistry, Faculty of Science, El-Menoufia University, Shebin El-Kom, Egypt

ARTICLE INFO

Article history:
Received 4 August 2010
Received in revised form
29 September 2010
Accepted 18 October 2010

Keywords:
Macrocyclic ligand
Copper(II) complexes
Spectral studies
Thermal analysis (TG/DTG)
Antitumor activity
DFT calculations

ABSTRACT

A novel (N_6O_4) macrocyclic ligand (**L**) and its Cu(II) complexes have been prepared and characterized by elemental analysis, spectral, thermal (TG/DTG), magnetic, and conductivity measurements. Quantum chemical calculations have also been carried out at B3LYP/6-31+G(d,p) to study the structure of the ligand and one of its complexes. The results show a novel macrocyclic ligand with potential amide oxygen atom, amide and amine nitrogen atoms available for coordination. Distorted square pyramidal ([Cu(L)Cl]Cl·2.5H_2O (**1**), [Cu(L)NO_3]NO_3·3.5H_2O (**2**), and [Cu(L)Br]Br·3H_2O (**4**) and octahedral ([Cu(L)$(OAc)_2$]·5H_2O (**3**)) geometries were proposed. The EPR data of **1**, **2**, and **4** indicate d^1 x^2-y^2 ground state of Cu(II) ion with a considerable exchange interaction. The measured cytotoxicity for L and its complexes (**1**, **2**) against three tumor cell lines showed that coordination improves the antitumor activity of the ligand; IC_{50} for breast cancer cells are ≈8.5, 3, and 4 μg/mL for **L** and complexes (**1**) and (**2**), respectively.

1. Introduction

Design of new macrocyclic compounds of different sizes, structures and properties represents an active area of research due to their widespread applications in chemistry and biology [1–13]. These rings can accommodate a variety of metal ions depending on the cavity size, metal ion, and ring structure [10,12,13]. The coordination chemistry of several macrocyclic ligands has been the subject of many studies [2–11]. The most common route for preparation of Polyaza macrocycles is the condensation of primary diamines with dialdehydes, diketones or diesters [1,12–14]. One class of these macrocycles is those incorporating amide groups [1,3–6,8–10,12,13]. Due to the presence of proton donor (N–H) and proton acceptor (C=O), hydrogen bond formation is common in these macrocycles and affects their structures [1,6]. Hydrogen bonding is crucial for functionality of biological systems such as RNA, DNA, proteins, and enzymes. Therefore, many efforts have been devoted to design new molecules with potential hydrogen bonding to interact with these biological systems [1,3–6,8–10,12–15]. Macrocyclic compounds containing oxalamide moiety have been synthesized and showed a variety of catalytic and biological activities [1,8–10,12,13]. The amide groups can bind with different metal ions via nitrogen and/or oxygen atoms. Compounds incorporating metal atoms are known as antitumor drugs such as cisplatin [16].

Copper(II) ion is known to be involved in many biological processes [16,17] and its role in increasing antitumor efficacy of organic molecules was established [7,18–24]. However, to the best of our knowledge, the synthesis of a macrocyclic compound derived from the interaction of dipropylenetriamine with diethyloxalate has not been done so far. Therefore, this work reports the synthesis and characterization of the aforementioned compound and some of its Cu(II) complexes. This ligand represents a 22-membered (N_6O_4) macrocyclic molecule *viz* 1,4,8,12,15,19-hexaazacyclo-docosane-2,3,13,14 tetraone (**L**), Scheme 1. The structures of the targeted ligand and complexes were characterized by elemental analysis, spectral (IR, UV–Vis (MS, ^{1}H NMR for the ligand) and EPR) studies and thermal techniques, molar conductance and magnetic susceptibility measurements. Anticancer activity of L and its complexes (**1**, **2**) was also estimated. Quantum chemical calculations have been carried out to support and interpret experimental findings.

2. Experimental

2.1. Materials and methods

All chemicals and solvents were of analytical grade and were used as received.

2.1.1. Synthesis of the macrocyclic ligand

The (N_6O_4) ligand has been synthesized as described elsewhere for similar compounds [8,9,12,13]. A solution of diethyloxalate ((2 mL, 2.19 g, 15 mmol) in ethanol (60 mL) was added dropwise to a solution of dipropylenetriamine (2 mL, 2.21 g, 16.92 mmol)

* Corresponding author. Tel.: +20 16 4607974; fax: +20 48 2235689.
E-mail address: amelnahas@hotmail.com (A.M. El-Nahas).

1386-1425/$ – see front matter © 2010 Elsevier B.V. All rights reserved.
doi:10.1016/j.saa.2010.10.021

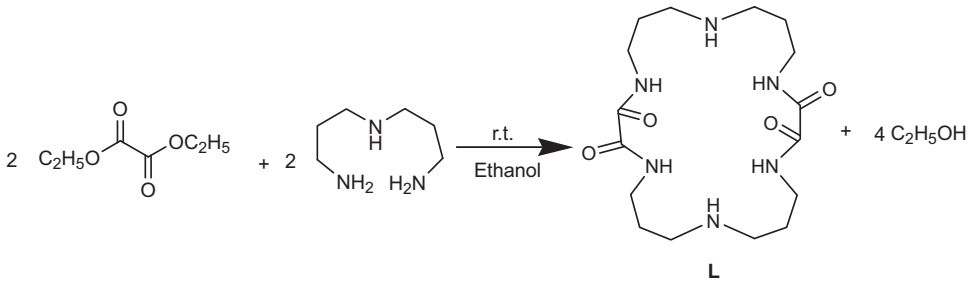

Scheme 1. Route of formation and suggested structure of the macrocyclic ligand (**L**).

in ethanol (70 mL) at room temperature and stirred vigorously overnight. The white precipitate formed (2.1 g, 50%) was filtered off and washed several times with cold EtOH and CH_3CN and vacuuo dried over P_4O_{10} (m.p. 190 °C).

2.1.2. Synthesis of the macrocyclic complexes

To a suspension of the macrocyclic ligand (0.5 g, 1.35 mmol) in 50 mL ethanol, a solution of hydrated copper(II) salt (chloride, nitrate, acetate or bromide for complexes 1, 2, 3 and 4, respectively) in 50 mL ethanol was added gradually, in molar ratio 1:1 (ligand: metal). The reaction mixture was heated under reflux for 8 h. The formed solid product was removed by filtration washed several times with ethanol and vacuuo dried over P_4O_{10}.

2.2. Physical measurements

The elemental analyses (C, H, N) were performed at Micro Analytical Center, Cairo University Giza, Egypt. Copper(II) content in the complexes was determined *via* iodometric method, while halide ions were determined by Volhard's method. Mass spectra (MS) were performed at the National Centre Institute, Egypt by the Thermo Electron Corporation. The Fourier Transform Infrared (FT-IR) measurements were performed (4000–400 cm^{-1}) in KBr discs using Nenexeus-Nicolidite-640-MSA FT-IR, Thermo-Electronics Co. The UV–visible absorption spectra were measured in Nujol mull using 4802 UV/vis double beam spectrophotometer. The ^1H NMR spectrum was recorded in DMSO d_6 using Varian Gemini 200 NMR spectrophotometer at 300 MHz. The electron paramagnetic resonance (EPR) spectra were recorded using a Varian E-109C model X-band spectrometer. The magnetic field modulation frequency was 100 kHz and the microwave power was around 10 mW. Molar conductivities were measured in DMSO solution of the complexes (10^{-3} M) using a CON 6000 conductivity meter, Cyberscan, Eutech instruments. Magnetic susceptibilities of the complexes were measured by the modified Gouy method at room temperature using Magnetic Susceptibility Johnson Matthey Balance. The effective magnetic moments were calculated using the relation $\mu_{eff} = 2.828(\chi_m T)^{1/2}$ B.M., where χ_m is the molar magnetic susceptibility corrected for diamagnetism of all atoms in the compounds using Selwood and Pascal's constants. Thermal analysis (TG/DTG) were obtained out by using a Shimadzu DTA/TG-50 Thermal analyzer with a heating rate of 10 °C /min in nitrogen atmosphere with a following rate 20 mL/min in the temperature range 30–800 °C using platinum crucibles.

2.3. Biological tests

Potential cytotoxicity of the ligand (**L**) and its complexes (**1**, **2**) was measured at the National Cancer Institute, Cairo University Egypt by SRB assay using the method of Skehan et al. [25]. Cells were plated in 96-multiwell plate (10^4 cells/well) for 24 h before the treatment with the target compounds to allow attachment of cell to the wall of the plate. Different concentrations of the compounds under test (0, 1, 2.5, 5 and 10 μg/mL) were added to the cell monolayer triplicate wells which were prepared for individual dose. Monolayer cells were incubated with the compounds for 48 h at 37 °C and in 5% CO_2 atmosphere. After 48 h, the cells were fixed, washed and stained with Sulfo-Rhodamine-B stain. Excess stain was washed with acetic acid and attached stain was recovered with Tris EDTA buffer. Color intensity was measured in an ELISA reader. The relation between the surviving fraction and the tested compound's concentration was plotted to get the survival curve of each tumor cell line for the specified compound.

2.4. Quantum chemical calculations

All electronic structure calculations were performed using the Gaussian03 suite of programs [26]. Geometry optimizations for the macrocyclic ligand and its complex (**1**) have been conducted without constraints using Density Functional Theory (DFT) at the B3LYP [27–29] functionals in conjunction with the 3-21G(d) basis set. Vibrational frequency calculations have been carried out at the same level of theory to characterize the optimized structures as minima or transition states and to correct energies for zero-point energy and thermal contribution. The vibrational modes were examined by using the ChemCraft program [30]. The calculated vibrational frequencies were scaled by 0.962 to account for the anharmonicity of the experimental frequencies. The calculations indicated that the ligand and complex (**1**) are minima (all eigenvalues of the force constant matrix are positive). Partial charge distributions were calculated using the natural population analysis (NPA) method [31]. Energies of all species were further refined at the B3LYP/6-31+G(d,p). Solvation effect has been modeled in ethanol using the polarized continuum model (PCM) of Tomasi and coworkers [32–35] at the B3LYP/6-31+G(d,p) level.

3. Results and discussion

The physical properties and analytical data of the ligand and its Cu(II) complexes were given in Table 1. The condensation of diethyloxalate with dipropylenetriamine gives the expected [2 + 2] tetraamide macrocyclic compound (**L**) (Scheme 1). The reaction of the macrocyclic ligand with the hydrated copper(II) chloride, nitrate, acetate or bromide in 1:1 molar ratio yielded the Cu(II) complexes (Scheme 2). The new compounds have been characterized by elemental analyses, spectral (IR, UV–Vis, EPR (MS, ^1H NMR for the ligand)), thermal analysis (TG/DTG) techniques, magnetic and conductivity measurements. The elemental analyses data are consistent with the proposed molecular formulas that show 1:1 metal to ligand ratio in these complexes. The novel green or blue copper(II) compounds are stable in air. The crystals were unsuitable for single-crystal X-ray structure determination and are insoluble in most common solvents, including ethanol, methanol, ethyl acetate, and acetonitrile. Complexes (**1**, **2**) are soluble in dimethyl-

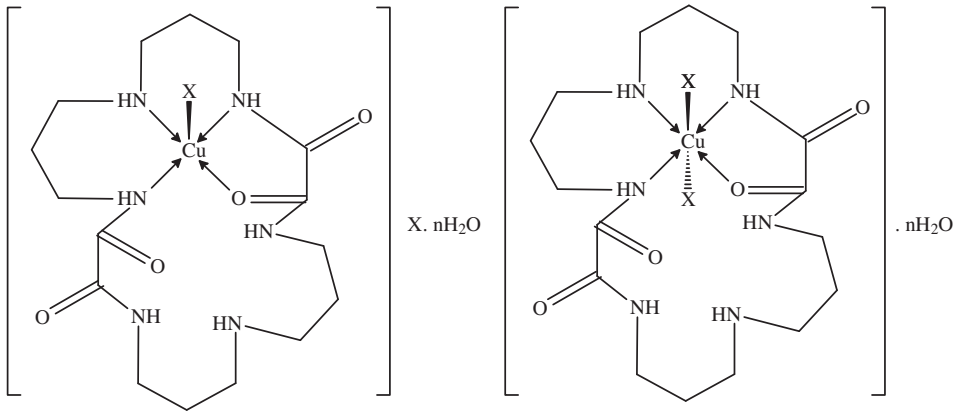

(1) X = Cl, n = 2.5
(2) X = NO_3, n = 3.5
(3) X = Br, n = 3

(4) X = OAc, n = 5

Scheme 2. Suggested structures of the complexes (**1**–**4**).

sulfoxide (DMSO) without change in color. Molar conductivity measurements of complexes (**1**, **2**) in 10^{-3} M DMSO solution are in the 58–72 Ω^{-1} cm^2 mol^{-1} range, correspond to 1:1 electrolyte [36]. With the exception of DMSO, the solubility of the macrocyclic ligand in other organic solvents is very limited. Intra- and/or intermolecular hydrogen bonds network is probably the key factor behind such limited solubility. It has been reported that hydrogen bond network could be a driving force in the formation of the [2 + 2] product [12].

3.1. Spectral studies

3.1.1. Mass spectra and ^1H NMR

The electrospray ionization (ESI) mass spectrum of the free ligand (**L**) in DMSO solution of approximately 10^{-4} M confirms the [2 + 2] macrocyclic form by observing a molecular ion peak at *m/z* 371 amu [MH^+] corresponds molecular formula of $C_{16}H_{30}N_6O_4$ (calculated *M* = 370). The mass spectrum of the free ligand also shows structurally important fragment ions at *m/z* 56 $[C_3H_6N]^+$, *m/z* 70 $[C_3H_7N_2]^+$, *m/z* 129 $[C_6H_{15}N_3]^+$, *m/z* 186 $[C_8H_{15}N_3O_2]^+$, *m/z* 299 $[C_{14}H_{29}N_5O_2]^+$, *m/z* 328 $[C_{15}H_{30}N_6O_3]^+$ and *m/z* 343 amu $[C_{15}H_{30}N_6O_3]^+$. The ^1H NMR spectrum of the free macrocyclic ligand shows a signal at δ 8.84 ppm attributed to amide (4H (br), CO–NH) and at δ 3.48 ppm (–CO–NH–CH_2). The signals appeared at δ 2.533 ppm and δ 1.633 ppm could be assigned to secondary amine (–CH_2–NH–CH_2–) and methylene protons, respectively.

3.1.2. Infrared spectra

Selected IR spectral bands for the ligand and its complexes are given in Table 2. The IR spectrum of the free ligand is characterized mainly by the strong bands at 3292, 1652, 1215, 1525, and 766 cm^{-1}, which are attributed to the stretching frequencies of NH (secondary amino group), amide-I ν(C=O), amide-III ν(C–N), and bending frequencies of amide-II δ(N–H), and amide-IV δ(C=O) bands, respectively [8,9]. This supports the macrocyclic nature of the ligand. There is another broad band at 3500 cm^{-1} due to the presence of lattice water molecules. The alkyl CH_2 group shows characteristic stretching absorption bands in the region 2943 cm^{-1}, deformation band at 1442 cm^{-1} and rocking modes at 677 cm^{-1}, respectively. The bonding of the ligand to copper(II) has been judged by a careful comparison of the infrared spectra of the complexes with that of the free ligand. In general, the IR spectra of the complexes exhibit merged and broadened bands compared to the sharp bands of free ligand. The ν(O–H) band of free ligand was observed at 3500 cm^{-1}, while on complexation a broad band at ca. 3459–3407 cm^{-1} was found indicating the presence of crystallized water molecules. Additionally, bands at ca. 3407–3300 cm^{-1} recorded for the complexes, were attributed to the overlap of free and coordinated ν(N–H) of secondary amido/amino groups of the ligand [13]. The stretching frequencies of the amide-I ν(C=O) groups in the complexes appear in two separate regions. The first region was observed at 1628–1602 cm^{-1} which is lower than the ν(C=O) of the free ligand (1652 cm^{-1}). This low shift, may be ascribed to the coordination of the C=O group to the metal ion. The second region located at 1660–1658 cm^{-1} is nearly at the same stretching frequency of the free ligand (1652 cm^{-1}). This indicates the presence of uncoordinated C=O groups.

It is noticed that the IR absorptions of complexes show a high frequency shift for coordinated ν(N–H) and a low shift for coordinated ν(C=O) compared to the ligand (Table 2). This behavior reveals that the electronic density of nitrogen is more delocalized with the carbonyl group in the complexes than in the ligand [1]. The IR spectra of the complexes also show that the amide II δ(N–H) recorded at 1525 cm^{-1} in the free ligand, is shifted to a lower frequency (1520–1510 cm^{-1}) and that amide III, ν(C–N) occurs at 1215 cm^{-1} in the free macrocycle ligand is shifted to higher frequency (1226–1225 cm^{-1}) supporting coordination through the C=O group. A further evidence for these coordination modes is the appearance of new two peaks at 530–508 and 483–425 cm^{-1} due to ν(Cu–O) and ν(Cu–N) stretching vibrations, respectively. The IR spectrum of complex (**2**) displays an absorption band at 1385 cm^{-1} characterizing the free nature of the nitrate ion; the presence of ionic nitrate is also supported by conductance measurements [13,36–41]. Complex (**2**) exhibits also bands around 1430, 1340, and 1040 cm^{-1} corresponding to monodentate nitrate group [36–41]. The acetato complex (**3**) displays two bands at 1575 and 1380 cm^{-1} assignable to $\nu_{as}(COO^-)$ and $\nu_s(COO^-)$. This difference of 195 cm^{-1} confirms the monodentate nature of the coordinated acetate [42]. Therefore, and according to the IR spectra, it is concluded that the current macrocyclic ligand behaves as a neutral tetradentate ligand binds to the metal ion *via* two amide nitrogens, one secondary nitrogen atom, and one amide oxygen atom.

3.1.3. Electronic spectra and magnetic moment

The tentative assignments of the significant electronic spectral bands of complexes are presented in Table 3. The electronic spectrum of L in Nujoll mulls as well as in DMSO show absorption bands at 230, 330–290 nm, are due to n–π^* electronic transitions

Table 1
Analytical and physical data for the macrocyclic ligand and its Cu(II) complexes.

No.	Compound	Color	Empirical formula	Yield (%)	Decomp. Temp (°C)	Analysis Calc. (*F*) (%)					$\Lambda_m\ \Omega^{-1}\ cm^2\ mol^{-1}$
						C	H	N	M	Halogen	
	Ligand (L·2H_2O)	White	$C_{16}H_{34}N_6O_6$	50	195	47.29 (48.41)	8.3 (8.49)	20.6 (20.52)	–	–	–
1	[Cu(L)Cl]Cl·2.5H_2O	Green	$C_{16}H_{35}N_6O_{6.5}Cu$	75.3	200	34.9 (35.1)	6.3 (6.06)	15.2 (15.04)	11.56 (11.7)	12.9 (12.42)	58.3
2	[Cu(L)NO_3] NO_3·3.5H_2O	Green	$C_{16}H_{37}N_8O_{13.5}Cu$	92.3	200	30.94 (30.91)	5.96 (5.84)	18.3 (17.82)	10.2 (10.00)	–	72.27
3	[Cu(L)$(OAc)_2$] 5H_2O	Dark blue	$C_{20}H_{46}N_6O_{13}Cu$	75	193	37.14 (37.77)	7.22 (7.65)	14.41 (14.77)	9.90 (9.90)	–	Insoluble
4	[Cu(L) Br]Br·3H_2O	Green	C16H36N6O7Cu	90	200	29.90 (29.00)	5.4 (5.64)	12.96 (12.58)	9.80 (10.20)	24.66 (24.1)	Insoluble

Table 2
Important IR spectral bands (cm^{-1}) of the macrocyclic ligand and its copper(II) complexes.

No.	Compound	ν(O–H)	ν(N–H)	ν(C=O) amide I free	ν(C=O) amide I coord.	δ(N–H) amide II	ν(C–N) amide III	δ(C=O) amide-IV	ν(M–O)	ν(M–N)	Anion (NO_3^-, OAc^-)
	L·2H_2O	3500	3292	1652	–	1525	1215	766	–	–	–
1	[Cu(L)Cl]Cl·2.5H_2O	3412	3304	1658	1602	1517	1226	762	510	462	–
2	[Cu(L)NO_3]NO_3·3.5H_2O	3428	3300	1660	1602	1520	1225	754	508	425	(1385, 820)[a] (1430, 1340)[b]
3	[Cu(L)$(OAc)_2$]·5H_2O	3459	3415	1660	1628	1510	1225	755	520	450	(1575, 1380)[c]
4	[Cu(L)(Br)]Br·3H_2O	3407	3300	1660	1602	1516	1225	739	530	483	–

[a] Ionic nitrate.
[b] Monodentate nitrate.
[c] Monodentate acetate.

Table 3
EPR, bonding parameters, electronic spectral bands and magnetic moments of Cu(II) complexes.

Parameter	Complex			
	1	2	3	4
$g_{//}$	2.21	2.22	–	2.210
$g_{\perp}$	2.06	2.07	–	2.06
g_{av}[a]	2.11	2.12	–	2.11
g_{iso}	–	–	2.09	–
G	3.631	3.236	–	3.134
$K^2_{//}$	0.47	0.51	–	0.49
$K^2_{\perp}$	0.82	0.90	–	0.90
K^2	0.70	0.77	–	0.76
ΔE_2 (cm^{-1})	15,197	15,384	–	15,384
ΔE_3 (cm^{-1})	24,691	22,222	–	22,222
$A_{//}$ (gauss)	–	88.0	–	118
$A_{\perp}$ (gauss)	–	52.0	–	60
A_{av} (gauss)	–	63.4	–	79.3
f (cm)	–	248	–	182
α^2	–	0.53	–	0.61
β^2	–	0.96	–	0.80
γ^2	–	1.68	–	1.47
d–d transitions (nm)	658(br), 405	650(br), 450	800(s), 475	650(br), 450
Other transitions (nm)	380(s) 335, 250	370–350(s), 290	370(s), 260(s)	380–370(s), 230
(μ_{eff}) (B.M.)	1. 57	1.58	1.80	1.32

[a] $g_{av} = 2g_{\perp} + g_{//}/3, \quad 3K^2 = 2K^2_{\perp} + K^2_{//}$.

[2]. The geometry of the copper(II) complexes has been deduced from the electronic and EPR spectra and further supported by quantum chemical calculations. The electronic spectra of complexes (**1**, **2**, **4**) display bands around 658–650 and 450–405 nm which are indicative of distorted square pyramidal geometries, These bands may be assigned to the transitions $^2B_{1g} \rightarrow {}^2A_{1g}$ and $^2B_{1g} \rightarrow {}^2E_g$ [42]. The electronic spectra of complexes (**1**, **2**) in DMSO also show the same absorption spectra indicating that the structure is not affected by solvent. The acetato complex (**3**) exhibits band around 800 and near 475 nm corresponding to distorted octahedral geometry. These bands may be assigned to $^2B_{1g} \rightarrow {}^2B_{2g}$ and $^2B_{1g} \rightarrow {}^2E_g$ transitions, respectively [3]. Additional peaks observed at higher energy were assigned to intra-ligand transitions. The room temperature magnetic moments measurements of the complexes are given in Table 3. The expected range for magnetically diluted Cu(II) complexes extended between 1.7 and 2.2 B.M. Complexes with the magnetic moments below this range indicate antiferromagnetic coupling [43]. Although complex (**4**) has a mononuclear structure, it shows subnormal value (1.32 B.M.) which may be attributed to intermolecular copper–copper interaction [43–45].

3.1.4. EPR spectra

EPR spectra of Cu(II) complexes provide information about the coordination environment around copper(II) ion [43,45]. The solid state EPR spectra of the copper(II) complexes (**1**–**4**) were recorded at room temperature on the X-band frequency 9.71 GHz. The EPR parameters observed for the powdered complexes are listed in Table 3. With the exception of complex (**3**), the EPR spectra of other Cu(II) complexes on the high field side are more intense than the low field side, indicating a d_{x2-y2} ground state for the copper(II) ion. Analysis of the spectra gives $g_{//} = 2.22–2.12$ and $g_{\perp} = 2.07–2.06$ (Table 3). The trend $g_{//} > g_{\perp} > 2.0023$, observed for the complexes under investigation also suggests d_{x2-y2} ground state for the Cu(II) ion [46–48]. The greater value of $g_{//}$ compared to $g_{\perp}$ proposes a distorted square pyramidal structure and rules out the possibility of a triagonal bipyramidal structure which is expected to have $g_{\perp} > g_{//}$ [49,50]. Also, the observed $g_{//}$ values of less than 2.3 provide evidence for the covalent character of bonding between Cu(II) ion and the ligand [51]. The exchange interaction between the copper centers in polycrystalline sample is explained by Hathaway expression $G = g_{//} - 2.0023/g_{\perp} - 2.0023$ [52]. The exchange interaction is neg-

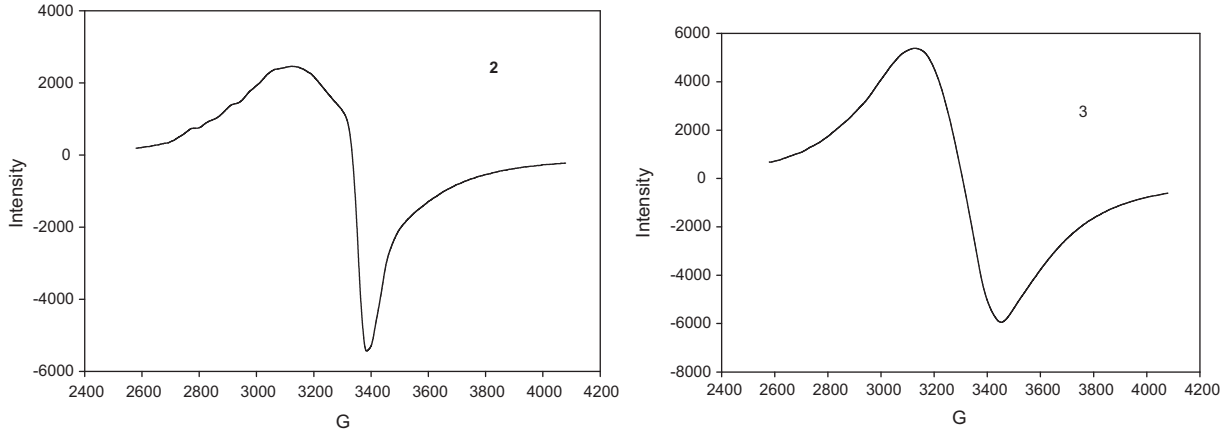

Fig. 1. EPR spectra of complexes (**2**, **3**) as polycrystalline sample at RT.

Table 4
Thermal data of the investigated compounds.

No	Compound	Temperature range (°C) DTG	TG	Mass loss% Calc.	(F.)	Reaction	Leaving species
	Ligand ($L{\cdot}2H_2O$)	163, 190	30–195	8.80	(8.8)	(i)[a]	$-2H_2O$
		339, 557	195–625	91.2	(91.2)	(ii)[b]	Decomposition
1	$[Cu(L)Cl]Cl{\cdot}2.5H_2O$	55	30–100	8.16	(8.18)	(i)[a]	$-2.5H_2O$
		298, 569	200–700	67.3	(67.3)	(ii)[b]	–ligand($C_{16}H_{30}N_6O_4$)
			at 700	24.48	(24.52)[c]		$\equiv CuCl_2$
2	$[Cu(L)NO_3]\ NO_3{\cdot}3.5H_2O$	50	30–130	7.2	(6.7)	(i)[a]	$-2.5H_2O$
		178	154–200	2.9	(2.9)	(i)	$-H_2O$
		260, 426	200–501	74.9	(74.5)	(ii)[b]	Gradual decomposition
			at 501	14.7	(14.8)[c]		$\equiv CuO_{1.5}$
3	$[Cu(L)(OAc)_2]{\cdot}5H_2O$	50	30–190	14.0	(14.0)	(i)[a]	$-5H_2O$
		268, 530	193–613	66.8	(67.0)	(ii)[b]	Gradual decomposition
			at 613	19.19	(19.0)[c]		$\equiv Cu(OAc)$
4	$[Cu(L)\ Br]Br{\cdot}3H_2O$	50	30–101	8.33	(8.00)	(i)[a]	$-3H_2O$
		301, 376, 694	200–724	81.87	(82.4)	(ii)[b]	Loss of $C_{16}H_{30}N_6O_4Br_2$
			at 724	9.81	(9.60)[c]		$\equiv Cu$

[a] Dehydration.
[b] Decomposition.
[c] Final product percent.

ligible if $G > 4$, whereas a considerable interaction occurs for $G < 4$. As shown in Table 3, the calculated G values for copper(II) complexes (**1**, **2**, **4**) are less than 4 suggesting some interaction between Cu(II) ions in the solid state, which is further confirmed by their subnormal magnetic moments values.

Complexes (**2**) (Fig. 1) and (**4**) show hyperfine anisotropy EPR spectra with well-defined hyperfine structure on the low field region due to the interaction between the unpaired electron of Cu(II) ion with its nucleus This allows accurate calculations of $g_{//}$ and $A_{//}$ values that are used to determine the empirical factor $f = g_{//}/A_{//}$, which is used as an index for tetragonal distortion [53–55]. The value of f from 105 to 135 cm indicates square-planar structures whereas larger values reveal tetragonally distorted complexes [53]. The f values for the investigated complexes given in Table 3 indicate distorted square pyramidal geometry. The EPR parameters $g_{//}$, $g_{\perp}$, g_{av}, $A_{//}$ (Cu) and $A_{\perp}$ (Cu) and the energies of d–d transitions were used to evaluate the bonding parameters α^2, β^2 and γ^2 which are used as measures of covalency of in-plane σ bonding, in-plane and out-of- plane π-bonding, respectively. The parameter α^2 is calculated from the following relation [51,56]:

$$\alpha^2 = \frac{A_{//}}{0.036} + (g_{//} - 2.0023) + \frac{3}{7}(g_{\perp} - 2.0023) + 0.04$$

The orbital reduction factors ($K_{//}^2 = \alpha^2\beta^2$ and $K_{\perp}^2 = \alpha^2\gamma^2$) which are the parallel and perpendicular components of orbital reduction factor also, give significant information about the nature of the bonding in copper complexes, they can be calculated using these expressions,

$$K_{//}^2 = \frac{(g_{//} - 2.0023)\Delta E_2}{8\lambda_o}$$

$$K_{\perp}^2 = \frac{(g_{\perp} - 2.0023)\Delta E_3}{2\lambda_o}$$

where λ_o is the spin-orbit coupling constant ($\lambda_o = -828\ cm^{-1}$ for free Cu(II) ion) and $\Delta E_2 = {}^2B_{1g} \rightarrow {}^2A_{1g}$, $\Delta E_3 = {}^2B_{1g} \rightarrow {}^2E_g$.

Complexes with $K_{//} < K_{\perp}$ imply a considerable in-plane π-bonding, while those with $K_{//} > K_{\perp}$ indicate an out-of-plane π bonding [57]. In complexes (**2**, **4**), $K_{//} < K_{\perp}$ and $K < 1$ indicates the presence of significant in-plane π bonding and greater covalent character for M–L bonding. However, the bond between Cu(II) ion and the ligand in-plane σ bond is purely ionic if $\alpha^2 = 1$ and entirely covalent if $\alpha^2 = 0.5$ [58]. The complexes under investigation give $\alpha^2 = 0.53–0.61$ indicating high covalency in these complexes. On the other hand, the values of β^2 (0.96–0.80) reflect the presence of in-plane π-bonding. The γ^2 values of 1.47–1.68 show an ionic character of the out-of-plane-π-bonding [58]. Complex (**3**) exhibits isotropic EPR spectrum with intense broad signal without hyperfine structure, Fig. 1. This is attributed to exchange interaction which would be mainly dipolar in character between the copper ions of the neighboring molecules and unresolved hyperfine interaction in the solid state [59].

3.2. Thermal analysis

The thermal properties of the current macrocyclic ligand and its copper(II) complexes were investigated by thermogravimetric analysis (TGA) and differential thermogravimetry (DTG), under nitrogen atmosphere from 30 to 800 °C; important data are summarized in Table 4.

3.2.1. Ligand

For the macrocyclic ligand, the TGA curve shows weight loss of 8.8% (theoretical. 8.8%); in the temperature range of 30–195 °C. The two weak endothermic DTG peaks recorded at 163 and 190 °C reflect the loss of two water molecules per ligand molecule. These results agree well with the composition of the ligand determined from elemental analysis and IR spectrum. The TG curve indicates a thermal stability till 195 °C which coincides with the melting point of the ligand (190 °C). The TG curve also shows two decomposition steps (Fig. 2) in the temperature range 190–625 °C, with total weight loss of 100.0% (found 100.0%), for the first and second steps. These weight losses may be ascribed to the successive loss of $C_{16}H_{30}N_6O_4$ molecule as gases at the given temperature range, coincide with DTG curve which shows peaks maximum at 339 and 557 °C.

3.2.2. Complexes

Fig. 2 represents TG/DTG curves of the complexes (**1**–**4**). The corresponding data are summarized in Table 4. The thermal behavior of all complexes is almost similar. For complexes (**1**, **2**, **4**), The TG curves show weight loss in the temperature range 30–190 °C, associated with one endothermic DTG peak at 50–55 °C. This was assigned to loss of water of crystallization in one step (Table 4), the lower onset of dehydration processes (30 °C) together with its extended range of temperatures indicate physical bonding for

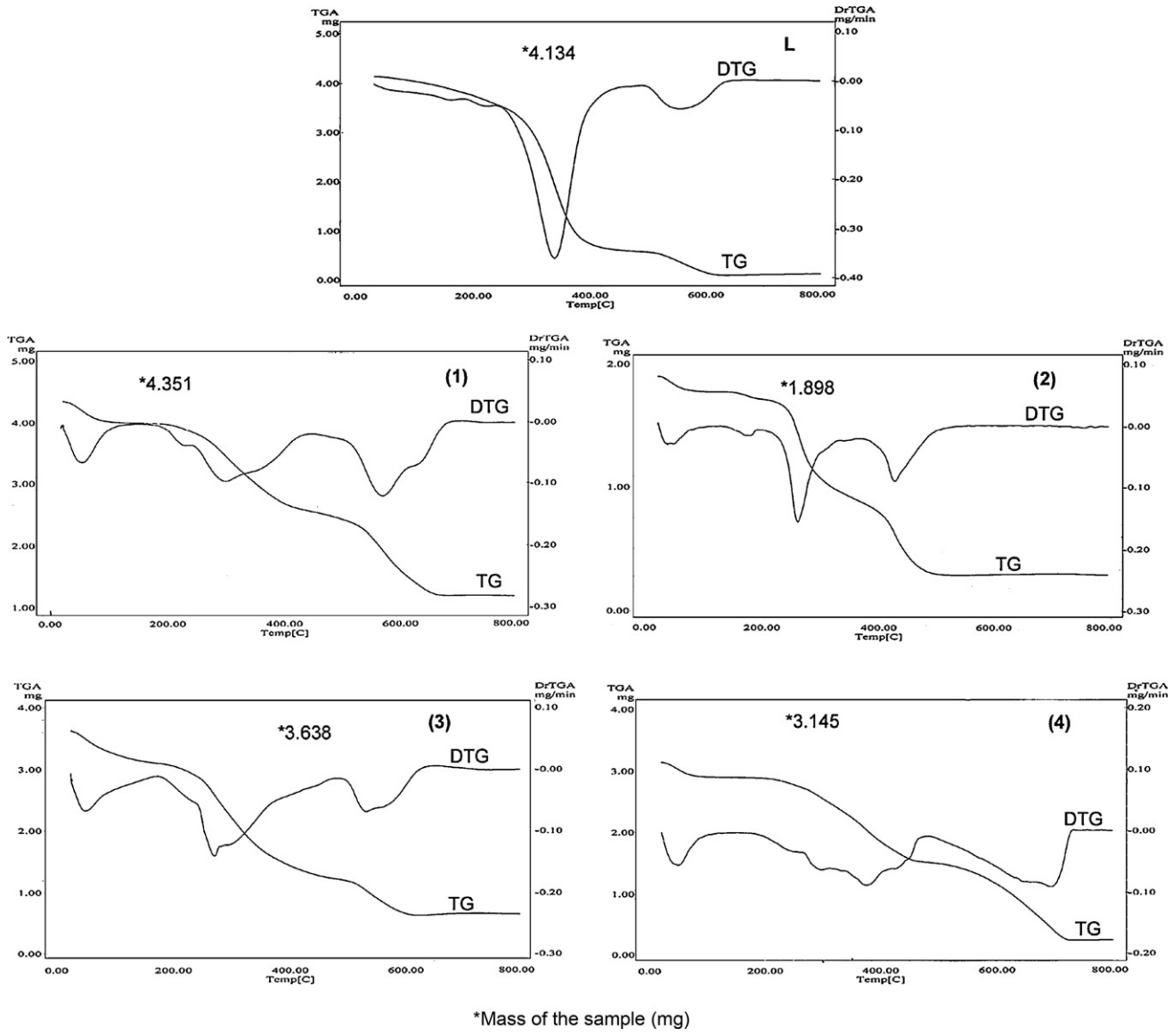

Fig. 2. TG/DTG curves of the macrocyclic ligand and its copper(II) complexes (**1**–**4**).

water of crystallization [60–64]. For Complex (**2**), the TG curve shows also weight loss of 2.9% (theoretical.2.9%), in the range of 154–200 °C, associated with endothermic DTG peak at 178 °C. This was assigned to loss of the last water molecule. As seen on hot stage microscope, the complex decomposes at 200 °C; the relatively high value of the temperature of the second dehydration step for complex (**2**) indicates strong water-lattice interaction. For complex (**3**), The TG curve shows weight loss in the temperature range 30–190 °C, associated with one endothermic DTG peak at 55 °C that was assigned to loss of five molecules of water of crystallization in one step (Table 4). As the temperature is increased; complexes degrade only in two steps. This degradation is due to pyrolysis of the organic ligand molecule. On the basis of elemental analysis, molar conductance measurements, magnetic susceptibilities, different spectra, thermal data, and the discussion given above, the suggested structures for the complexes (**1**–**4**) are given in Scheme 2.

3.3. DFT calculations

Because of our unsuccessful trails to get crystalline samples for X-ray crystallography, DFT calculations have been conducted for better understanding of the structures of the macrocyclic ligand and complex (**1**). The optimized structures of the ligand and complex (**1**) are displayed in Fig. 3.

The complex (**1**) adopts a square pyramidal structure with the Cu(II) ion coordinated to two amide nitrogen atoms, one amine nitrogen atom, and one oxygen atom. These four atoms form a distorted plane with the Cl atom located at the *z*-axis. The angular structural parameter τ [65,66] defined as the difference between the O1CuN6 (159.6°) and N4CuN5 (133.3°) angles divided by 60° equals 0.44 compared to 1 for equilateral bipyramid and 0 for square pyramid. Moreover, the sum of bond angles around Cu atom is 344° which implies a pyramidalization degree of 16°. Starting the optimization process with an octahedral configuration for complex (**1**) leads gradually to the distorted square pyramidal structure with one of the Cl anions leaving the first coordination sphere to attach with one of the O–H of water and N4–H via hydrogen bonds in the second shell. All these observations support the experimental assignment of the distorted square pyramidal structure of the complex (**1**).

As depicted in Fig. 3, the optimized lengths for Cu–N5, Cu–N6, Cu–N4, Cu–O1, and Cu–Cl_{coord} are 1.989, 1.925, 2.055, 1.996, and 2.322 Å, respectively. The second Cl atom is located outside the first coordination sphere with the Cu–$Cl_{uncoord}$ bond distance of

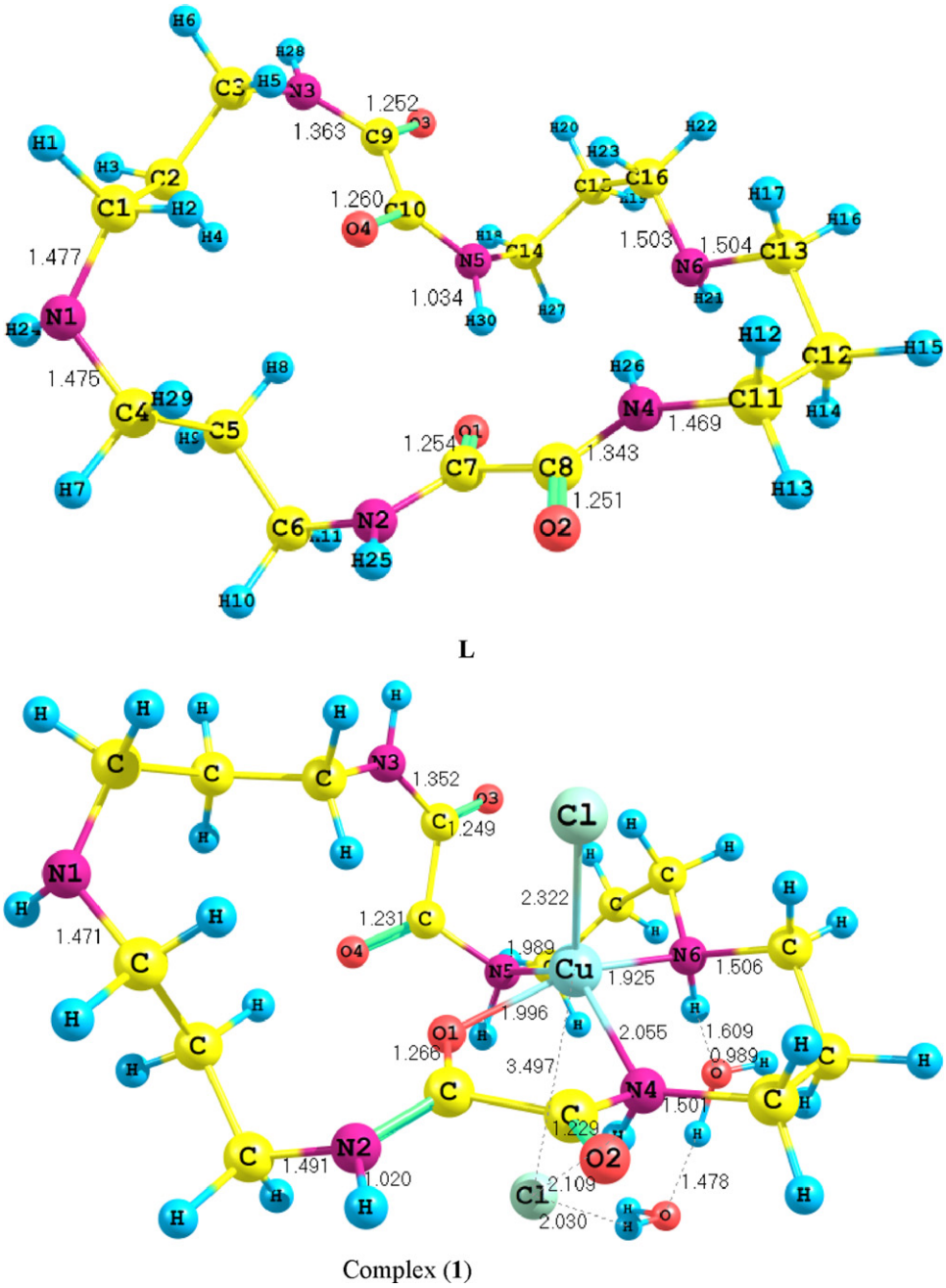

Fig. 3. Optimized structures of the ligand and complex (**1**) at B3LYP/3-21G(d).

3.495 Å. This Cl forms two hydrogen bonds with amide N4–H and water O–H bonds of 2.019 and 2.030 Å, respectively. A comparable geometrical parameters were reported previously for other complexes where Cu(II) is coordinated to nitrogen and oxygen atoms at B3LYP/6-31G, B3LYP/LanL2DZ, and B3PW91/LanL2DZ levels [67,68].

In order to shed light into the electronic structures of the ligand and its complex (**1**), natural bond orbital (NBO) analysis was carried out. Charges on all atoms were calculated from natural population analysis (NPA). NPA charges over nitrogen and oxygen atoms in the ligand and its copper(II) complex and the electron configuration of Cu(II) ion are listed in Table 5. The negative charge on nitrogen atoms are larger than on oxygen atoms. Therefore, it is expected that copper(II) ion will bind preferably with nitrogen atoms than with oxygen atoms unless the formers are hindered from coordination for steric reasons. In general, the negative charge on amine nitrogen is more than on the amide nitrogen because the electrons on the latter are resonating with the adjacent carbonyl group. This gives rise to a shorter Cu–N_{amine} bond compared to Cu–N_{amide}.(1.925 vs. 1.989 or 2.055 Å, respectively). From the second order perturbation NBO energy analysis, it has been shown that the strength of interaction of the Cu(II) ions with donor atoms decreases in the order Cl > N_{amine} > N_{amide} > N_{amide} > O; 39, 24, 20, 17, and 15 kcal/mol, respectively.

The charge on the Cu(II) ion in the complex (**1**) of 1.515 e is lower than its value in the free ion of +2e. This indicates a charge transfer from the ligands (**L**, Cl^-) to the central ion. The nitrogen and oxygen atoms acquired more negative in the complex while the positive charges on amine and amide hydrogen atoms are increased upon complexation. The increase of the positive charges on these hydrogen atoms might help in forming strong hydrogen bonds with biological molecules.

Table 5
Electron population and NPA charges at B3LYP/3-21G(d).

AO	Electron population		Atom[a]	NPA charges	
	Free Cu(II)	Complex (**1**)		L	Complex (**1**)
1s	2	2	Cu		1.515
2s	2	1.99999	N5	−0.634	−0.831
3s	2	1.99928	N6	−0.690	−0.844
4s	0	0.39037	N4	−0.642	−0.826
$2p_x$	2	1.99998	O1	−0.590	−0.661
$2p_y$	2	1.99998	Cl_{coord}		−0.833
$2p_z$	2	1.99998	$Cl_{uncoord}$		−0.757
$3p_x$	2	1.99925			
$3p_y$	2	1.99928			
$3p_z$	2	1.99943			
$4p_x$	0	0.03146			
$4p_y$	0	0.03881			
$4p_z$	0	0.03974			
$3d_{xy}$	2	1.63644			
$3d_{xz}$	2	1.9201			
$3d_{yz}$	2	1.79722			
$3d^{x2-y2}$	2	1.78832			
$3d^{z2}$	1	1.82461			
No. electrons	27	27.46424			
$3d_{total}$	9	8.96669			
NPA Charge	2	1.5			

[a] Atoms numbering system is given in Fig. 3.

Table 6
Selected vibrational modes and IR of ligand and its copper(II) complex (**1**).

Mode	Ligand		Complex (1)	
	Calcd.	Exp.	Calcd.	Exp.
ν(N–H)	3120–3390	3292(br)[a]	3361–3129 3127[b]	3304(br)[a]
ν(C=O)	1614–1652	1652(br)[a]	1661–1691 1633[b]	1658 1602[b]
ν(Cu–O) + ν(Cu–N)			535–370	510–462

[a] Broad band centered at this position.
[b] Groups coordinated with copper.

Table 7
Energies (eV) of frontier molecular orbitals (HOMO, LUMO) of the ligand and complex (**1**).

Compound	HOMO	LUMO	ΔE
Ligand (**L**)	−4.87	−0.64	4.23
Complex (**1**)	−5.03	−2.19	2.84

The calculated and experimental vibrational frequencies are collected in Table 6. The computed N–H and C=O stretching vibrational modes of the ligand of 3120–3390 cm^{-1} and 1614–1652 cm^{-1} match well with the corresponding experimental values at 3292 cm^{-1} and 1652 cm^{-1}. In the complex (**1**), the stretching N–H and C=O modes are shifted to higher and lower values, respectively. Theoretically, the coordinated N–H and C=O bonds are shifted toward lower frequencies compared to the uncoordinated ones on the other side of the ligand.

The frontier molecular orbital energies of the ligand and complex (**1**) are listed in Table 7. The highest occupied molecular orbital (HOMO) and the lowest unoccupied molecular orbital (LUMO) represent a means of measuring electron donating or accepting ability of a given molecular system, respectively. The LUMO in complex (**1**) is strongly stabilized and, therefore, the energy gap ($\Delta E = E_{LUMO} - E_{HOMO}$) is relatively lower than in the ligand suggesting a strong activity of the former [69].

The calculated binding energies of the complex (**1**) in the gas phase and ethanolic solution at different levels of theory are given in Table 8. It is clear that the calculations in ethanol decrease the binding energy by 3–4 times due to the high electrostatic stabilization of the free Cu(II) ion in ethanol solution compared to the complex itself.

Table 9
Lethal concentration (IC_{50}) of the macrocyclic ligand and its copper(II) complexes on different cell lines.

No.	Compound	IC_{50} (μg/mL)		
		HCF7	HEPG2	HCT 116
	(L·2 H_2O)	8.46	13.9	17.3
1	[Cu(L)Cl]Cl 2.5H_2O	2.82	3.28	3.74
2	[Cu(L)NO_3]NO_3 3.5H_2O	3.89	3.43	4.19

3.4. Biological activity

The biological activities of the macrocyclic ligand and its complexes (**1**, **2**) (tested at the National centre Institute, Cairo University Egypt) were detected by SRB assay. The results of these experiments are collected in Table 9 and plotted in Fig. 4 The pharmacological testing has proved that the ligand and its copper (II) complexes (**1**, **2**) show excellent anticancer activity toward breast cells (HCF7), human hepatocarcinoma HEPG2 cells and colon carcinoma cells (HCT116). The measured cytotoxicity for the macrocyclic ligand and its complexes (**1**, **2**) against three tumor cell lines shows that coordination improves the antitumor activity of the new ligand. For breast cancer cells, the IC_{50} values are ~8.5, 3, and 4 μg/mL for the ligand, complexes (**1**) and (**2**), respectively. The other two cancer cells give similar or slightly less activity. The enhanced activity of the investigated complexes agree with the documented activity of copper(II) complexes as antitumor agents [7,19,20,18,21–24]. Our reported values for complexes (**1**) and (**2**) for breast cancer

Table 8
Energies (X) of Cu(II), H_2O, Cl^-, ligand, and complex (**1**) in the gas phas and ethanolic solution at B3LYP/basis sets.

X/Level	Ligand (au)	Cl^- (au)	H_2O (au)	Cu(II) (au)	Complex (1) (au)	ΔX[a] (kcal/mol)
E_0/3-21G(d)	−1249.85612	−458.16037	−75.95421	−1631.51161	−3950.83063	−774.19
E_{298}/3-21G(d)	−1249.83008	−458.15896	−75.95137	−1631.51020	−3950.79543	−774.66
H_{298}/3-21G(d)	−1249.82914	−458.15801	−75.95043	−1631.51020	−3950.79449	−777.03
G_{298}/3-21G(d)	−1249.91184	−458.17539	−75.97195	−1631.49576	−3950.89653	−749.40
E_0/6-31+G(d,p)	−1256.81514	−460.27473	−76.41261	−1639.25153	−3970.46602	−643.00
E_{298}/6-31+G(d,p)	−1256.78910	−460.27331	−76.40978	−1639.25011	−3970.43082	−643.47
H_{298}/6-31+G(d,p)	−1256.78816	−460.27237	−76.40883	−1639.25011	−3970.42987	−645.84
G_{298}/6-31+G(d,p)	−1256.87086	−460.28975	−76.43036	−1639.23567	−3970.53192	−618.21
E_0/6-31+G(d,p) (in Ethanol)	−1256.85648	−460.38550	−76.42512	−1639.73609	−3970.51787	−190.89 (−494.87)[b]
E_{298}/6-31+G(d,p) (in Ethanol)	−1256.83044	−460.38408	−76.42228	−1639.73467	−3970.48266	−191.27 (−495.34)[b]
H_{298}/6-31+G(d,p) (in Ethanol)	−1256.82950	−460.38314	−76.42134	−1639.73467	−3970.48172	−193.64 (−497.71)[b]
G_{298}8/6-31+G(d,p) (in Ethanol)	−1256.91220	−460.40052	−76.44286	−1639.72023	−3970.583767	−166.01 (−470.08)[b]

[a] $X = E_0$, E_{298}, H_{298}, G_{298} (total energy corrected for zero-point energy, total energy at 298 K, enthalpy at 298 K, and free energy at 298 K), ΔX (binding energy) = ($X_{complex} - X_L - 2X_{H2O} - 2X_{Cl-}$).
[b] Calculated using unsolvated Cu(II) ion.

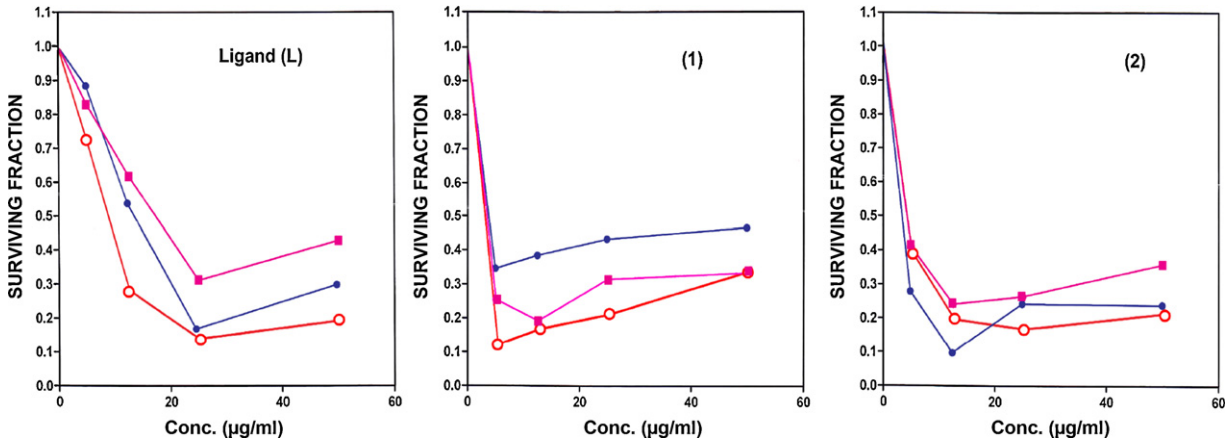

Fig. 4. Dose response curves of HCT116 (■), MCF7 (○), HEPG2 (●) cells after treatment with the ligand (**L**) and complexes (**1**, **2**).

cells are better than the values of 54–65 μg/mL for the same cells given by Cu(II) Schiff mono-base complexes with 2-thiophenecarboaldehyde and dipropylenetriamine [19].

The enhanced activity of the complex can be ascribed to some factors. First is the increasing hydrogen bond ability of the complex because of high positive charges on hydrogen atoms of the coordinated amide and amine groups; on average 0.44 vs. 0.41 e in the complex and ligand, respectively. Second is the high stability of LUMO in the complex shows a potential for oxidizing ability of the complex compared to the ligand, Table 7. It has been reported that some copper(II) complexes act on cancer cell through oxidative stress mechanism [7,70].

4. Conclusions

In this work, synthesis and characterization of a novel macrocyclic ligand and its copper(II) complexes (**1**–**4**) are reported. The analytical and physicochemical analysis confirmed the composition and the structure of the newly obtained compounds. The results obtained can be summarized as follows:

1. The new macrocyclic compound behaves as a neutral tetradentate ligand when reacts with different Cu(II) salts.
2. Mononuclear complexes are formed. They adopt distorted square pyramidal configurations with the chloride, bromide, and nitrate. However, the acetato complex prefers a distorted octahedral geometry.
3. Quantum chemical calculations support the experimental characterization of the structures of the ligand and complexes.
4. The pharmacological results suggest that the novel ligand and its copper(II) complexes are potent anticancer agents. Besides, the cytotoxicity of copper complexes is higher than that of the ligand, which implies an increase in the antitumor activity with coordination.

Acknowledgments

We would like to thank Professor Kimihiko Hirao (Riken, Wako, Japan) and Professor Tetsuya Taketsugu (Hokkaido University, Sapporo, Japan) for allocation of some computational facilities.

References

[1] E.F. Montero-Vázquez, F.J. Martínez-Martínez, I.I. Padilla-Martínez, M.A. Carvajal-García, J.H. Hernández-Díaz, ARKOVIC (V) (2008) 276–282.
[2] M. Salavati-Niasari, F. Davar, K. Saberyan, Polyhedron 29 (2010) 2149–2156.
[3] S. Chandra, L.K. Gupta, D. Jain, Spectrochim. Acta Part A 60 (2004) 2411–2417.
[4] R.M. Izatt, R.L. Bruening, B.J. Tarbet, L.D. Griffien, M.L. Bruening, K.E. Krakowiak, J.S. Bradshaw, Pure Appl. Chem. 62 (1990) 1115–1118.
[5] D.P. Singh, R. Kumar, J. Singh, Eur. J. Med. Chem. 44 (2009) 1731–1736.
[6] A. Chaudhary, R.V. Singh, Metal Based Drugs 8 (2002) 315–321.
[7] I. Dovinová, H. Pukíková, P. Rauko, L'.H. Ková, E. Hanušovská, E. Tibenská, Toxicology in Vitro 16 (2002) 491–498.
[8] S. Chandra, L.K. Gupta, Spectrochim. Acta Part A 60 (2004) 1563–1571.
[9] S. Chandra, L.K. Gupta, Spectrochim. Acta Part A 61 (2005) 2139–2144.
[10] M. Salavati-Niasari, J. Mol. Catal. A: Chem. 278 (2007) 22–28.
[11] V. Alexander, Chem. Rev. 95 (1995) 273–342.
[12] F. Denat, R. Tripier, F. Boschetti, E. Espinosa, R. Guilard, ARKIVOC (IV) (2006) 212–233.
[13] R. Tripier, O. Siri, F. Rabiet, F. Denat, R. Guilard, Tetrahedron Lett. 40 (1999) 79–82.
[14] J.S. Nowick, J.H. Tsai, Q.-C. Bui, S. Maitra, J. Am. Chem. Soc. 121 (1999) 8409–8410.
[15] C. Mcfarland, D.A. Vivic, A.V. Debnath, Synthesis 5 (2006) 807–812.
[16] H.M. Pinto, J.H. Schornagel (Eds.), Platinum and Other Metal Coordination Compounds in Cancer Chemotherapy 2, Plenum, New York, 1996.
[17] H. Kozłowski, T. Kowalik-Jankowska, M. Jèzowska-Bojczuk, Coord. Chem. Rev. 249 (2005) 2323–2334.
[18] Y. Zhang, L. Zhang, L. Liu, J. Guo, D. Wu, G. Xu, X. Wang, D. Jia, Inorg. Chim. Acta 363 (2010) 289–293.
[19] A.Th. Caviara, P.J. Cox, K.H. Repana, A.A. Pantazaki, K.T. Papazisis, A.H. Kortsaris, D.A. Kyriakidis, G.St. Nikolov, C.A. bolos, J. Inorg. Biochem. 99 (2005) 467–476.
[20] M.P. Sathisha, U.N. Shetti, V.K. Revankar, K.S.R. Pai, Eur. J. Med. Chem. 43 (2008) 2338–2346.
[21] M. Collins, D. Ewing, G. Mackenzie, E. Sinn, U. Sandbhor, S. Padhye, S. Padhye, Inorg. Chem. Commun. 3 (2000) 453–457.
[22] N.H. Gokhale, S.S. Padhye, S.B. Padhye, C.E. Anson, A.K. Powell, Inorg. Chim. Acta 319 (2001) 90–94.
[23] R.-M. Wang, N.-P. He, P.-F. Song, Y.-F. He, L. Ding, Z.-Q. Lei, Polym. Adv. Technol. 20 (2009) 959–964.
[24] K.G. Daniel, D. Chen, S. Orlu, Q.C. Cui, F.R. Miller, Q.P. Dou, Breast Cancer Res. 7 (2005) R897–R908.
[25] P. Skehan, R. Storeng, D. Scudiero, A. Monks, J. McMahon, D. Vistica, J.T. Warren, H. Bokesch, S. Kenney, M.R. Boyd, J. Natl. Cancer Inst. 82 (1990) 1107–1112.
[26] M.J. Frisch, G.W. Trucks, H.B. Schlegel, G.E. Scuseria, M.A. Robb, J.R. Cheeseman, J.A. Montgomery Jr., T. Vreven, K.N. Kudin, J.C. Burant, J.M. Millam, S.S. Iyengar, J. Tomasi, V. Barone, B. Mennucci, M. Cossi, G. Scalmani, N. Rega, G.A. Petersson, H. Nakatsuji, M. Hada, M. Ehara, K. Toyota, R. Fukuda, J. Hasegawa, M. Ishida, T. Nakajima, Y. Honda, O. Kitao, H. Nakai, M. Klene, X. Li, J.E. Knox, H.P. Hratchian, J.B. Cross, V. Bakken, C. Adamo, J. Jaramillo, R. Gomperts, R.E. Stratmann, O. Yazyev, A.J. Austin, R. Cammi, C. Pomelli, J.W. Ochterski, P.Y. Ayala, K. Morokuma, G.A. Voth, P. Salvador, J.J. Dannenberg, V.G. Zakrzewski, S. Dapprich, A.D. Daniels, M.C. Strain, O. Farkas, D.K. Malick, A.D. Rabuck, K. Raghavachari, J.B. Foresman, J.V. Ortiz, Q. Cui, A.G. Baboul, S. Clifford, J. Cioslowski, B.B. Stefanov, G. Liu, A. Liashenko, P. Piskorz, I. Komaromi, R.L. Martin, D.J. Fox, T. Keith, M.A. Al-Laham, C.Y. Peng, A. Nanayakkara, M. Challacombe, P.M.W. Gill, B. Johnson, W. Chen, M.W. Wong, C. Gonzalez, J.A. Pople, Gaussian 03, Revisions C.02 and D.02, Gaussian, Inc., Wallingford, CT, 2004.
[27] A.D. Becke, J. Chem. Phys 98 (1993) 5648–5652.
[28] C. Lee, W. Yang, R.G. Parr, Phys. Rev. B 37 (1988) 785–789.
[29] P.J. Stephens, F.J. Devlin, C.F. Chabalowski, M.J. Frisch, Phys. Chem. 98 (1994) 11623–11627.
[30] G.A. Zhurko, D.A. Zhurko, ChemCraft version 1.5, 2005.
[31] A.E. Reed, R.B. Weinstock, F.A. Weinhold, J. Chem. Phys. 83 (1985) 735–746.
[32] S. Miertus, E. Scrocco, J. Tomasi, J. Chem. Phys. 55 (1981) 117–129.
[33] J. Tomasi, M. Persico, Chem. Rev. 94 (1994) 2027–2033.
[34] R. Cammi, J. Tomasi, J. Comput. Chem. 16 (1995) 1449–1458.
[35] M. Cossi, V. Barone, R. Cammi, J. Tomasi, J. Chem. Phys. Lett. 255 (1996) 327–333.

[36] W.J. Geary, Coord. Chem. Rev. 7 (1971) 81–122.
[37] V.P. Singh, Spectrochim. Acta Part A 71 (2008) 17–22.
[38] S. Sharma, N. Barooah, J.B. Baruah, J. Mol. Catal. A: Chem. 229 (2005) 171–176.
[39] G.C. Vlahopoulou, D.I. Alexandropoulos, C.P. Raptopoulou, S.P. Perlepes, A. Escuer, T.C. Stamatatos, Polyhedron 28 (2009) 3235–3242.
[40] K. Nakamoto, Infrared Spectra of Inorganic and Coordination Compounds, 2nd Ed., Wiley Interscience, 1963, p. 172.
[41] M.S. Nair, R.S. Joseyphus, Spectrochim. Acta A 70 (2008) 749–753.
[42] K.S. Bharathi, S. Sreedaran, A.K. Rahiman, K. Rajesh, V. Narayanan, Polyhedron 26 (2007) 3993–4002.
[43] T. Rosu, E. Pahontu, C. Maxim, R. Georgescu, N. Stanica, G.L. Almajan, A. Gulea, Polyhedron 29 (2010) 757–766.
[44] F.A. Cotton, G. Wilkinson, Advanced Inorganic Chemistry, John Wiley and Sons, New York, 1972, p. 918.
[45] M.M. Hassanien, I.M. Gabr, M.H. Abdel-Rhman, A.A. El-Asmy, Spectrochim. Acta Part A 71 (2008) 73–79.
[46] S. Chandra, S. Gupta, J. Indian Chem. Soc. 82 (2005) 1087–1090.
[47] B.J. Hathaway, A.A.G. Tomlinson, Coord. Chem. Rev. 5 (1970) 1–43.
[48] O.I. Singh, M. Damayanti, N.R. Singh, R.K.H. Singh, M. Mohapatra, R.M. Kadam, Polyhedron 24 (2005) 909–916.
[49] S. Tyagi, B.J. Hathaway, J. Chem. Soc. Dalton Trans. (1981) 2029–2033.
[50] E. Viñuelas-Zahinos, M.A. Maldonado-Rogado, F. Luna-Giles, F.J. Barros-Garcia, Polyhedron 27 (2008) 879–886.
[51] D. Kivelson, R. Neiman, J. Chem. Phys. 35 (1961) 149–155.
[52] B.J. Hathaway, D.E. Billing, Coord. Chem. Rev. 5 (1970) 143–207.
[53] U. Sakagushi, A.W. Addison, J. Chem. Soc. Dalton Trans. (1979) 600–608.
[54] S.M.M. Romanowski, F. Tormena, V.A. Santos, M.F. Hermann, A.S. Mangrich, J. Braz. Chem. Soc. 15 (2004) 897–903.
[55] R.P. John, A. Sreekanth, M.R.P. Kurup, A. Usman, A.R. Ibrahim, H.-K. Fun, Spectrochim. Acta Part A 59 (2003) 1349–1358.
[56] A.H. Maki, B.R. McGarvey, J. Chem. Phys. 29 (1958) 35–38.
[57] A.L. Sharma, I.O. Singh, M.A. Singh, H.R. Singh, Transit. Met. Chem. 26 (2001) 532–537.
[58] S. Chandra, D. Jain, A.K. Sharma, Spectrochim. Acta Part A 71 (2009) 1712–1719.
[59] K.K. Narang, V.P. Singh, Transit. Met. Chem. 21 (1996) 507–511.
[60] H.A. El-Boraey, J. Therm. Anal. Calorim. 81 (2005) 339–346.
[61] H.A. El-Boraey, A.M. Donia, M.F. El-Samalehy, J. Anal. Appl. Pyrol. 73 (2005) 204–211.
[62] A.M. Donia, H.A. El-Boraey, M.F. El-Samalehy, J. Therm. Anal. Calorim. 73 (2003) 987–1000.
[63] H.A. El-Boraey, F.A. El-Saied, S.A. Aly, J. Therm. Anal. Calorim. 96 (2009) 599–606.
[64] H.A. El-Boraey, R.M. Abdel-Raham, E.M. Atia, K.H. Hilmy, Cent. Eur. J. Chem. 8 (2010) 820–833.
[65] A.W. Addison, T.N. Rao, J. Reedijk, J. Rijn, G.C. Verschoor, J. Chem. Soc., Dalton Trans. (1984) 1349–1356.
[66] B. Machura, A. Świtlicka, M. Wolff, J. Kusz, R. Kruszynski, Polyhedron 28 (2009) 1348–1354.
[67] B. Machura, A. Switlicka, R. Kruszynski, J. Kusz, R. Penczek, Polyhedron 27 (2008) 2513–2518.
[68] T. Shi, S. He, X. Wang, Y. Wang, Z. Tang, Z. Wen, J. Mol. Struct. Theochem. 732 (2005) 201–209.
[69] H.E. Feng, D. Ying-Yi, Z. Xiao-Feng, H. Ai-Dong, Z. Ling, Y. Shao-Ping, L. Zong-Chao, Chin. J. Cancer Res. 14 (2002) 76–78.
[70] F. Tisato, C. Marzano, M. Porchia, M. Pellei, C. Santini, Med. Res. Rev. 30 (2010) 708–749.